Dissolution Behavior of AlN in CaO–Al$_2$O$_3$-Based Slag

Xufeng Wang, Zaihui Xi, Qiangqiang Wang, Shengping He, and Xubin Zhang

Abstract Fe–Mn–Al–C steel can form AlN particles because of its high [Al] content (w[Al] = 8–12 wt%), which can affect the properties of slag during continuous casting. In this study, the dissolution behavior of AlN in a new CaO–Al$_2$O$_3$-based slag without SiO$_2$ was investigated by a static experiment method. Results demonstrated AlN rod could be dissolved in the liquid slag and it only reacted with Li$_2$O, which caused the increase of Al$_2$O$_3$ and the decrease of Li$_2$O in the slag. The interface between slag and AlN was examined by scanning electron microscopy, and the products near the slag side were Al$_2$O$_3$–CaO–BaO–CaF$_2$ complexes, while individual Al$_2$O$_3$ and AlN–Al$_2$O$_3$ complexes were dispersed near AlN side. Additionally, the viscosity and break temperature of the slag increased greatly with the increase of AlN. XRD showed the primary crystalline phase in the slag was 11CaO·7Al$_2$O$_3$·CaF$_2$. This work provided theoretical guidance for future application of the slag for high-Al steel.

Keywords Fe–Mn–Al–C steel · CaO–Al$_2$O$_3$-based slag · AlN · Dissolution behavior · Physical and chemical properties

Introduction

Fe–Mn–Al–C steel with high-Mn and high-Al contents ([Mn] = 20–30%, [Al] = 5–12%) has been widely used in the automobile field in recent years, due to its excellent weight loss and high strength properties field [1, 2]. However, the [Al] in steel reacts with the oxidizing components in slag would lead to the composition change and performance deterioration of the slag. Thereby restricting the production of high-Al steel by continuous casting (CC) process.

To settle the issue of steel-slag reaction to realize the CC production of high-Al steel, a new type of CaO–Al$_2$O$_3$–BaO–CaF$_2$–Li$_2$O non-reactive mold flux which

X. Wang · Z. Xi · Q. Wang (✉) · S. He · X. Zhang
College of Materials Science and Engineering, and Chongqing Key Laboratory of Vanadium–Titanium Metallurgy and Advanced Materials, Chongqing University, Chongqing 400044, China
e-mail: wtfwawj@163.com

Table 1 Compositions of mold flux

Slag samples	CaO	Al_2O_3	CaF_2	Li_2O	BaO
wt%	30.12	29.02	17.54	7.64	15.68

discarded all the oxides was proposed [3, 4]. The network structure of the slag system was mainly $[AlO_4]^-$ tetrahedron [5] with simple chain and layer structure [6]. In addition, compared with the traditional CaO–SiO_2-based slag, the slag system had better wettability with high-Mn high-Al steel, which was beneficial for the performance of lubricating shell by the slag melt [7]. According to the excellent properties of the CaO–Al_2O_3–BaO–CaF_2–Li_2O non-reactive slag, the slag system has a good potential application prospect for the CC production of high-Al steel.

In the high-Al steel with [Al] content up to 5–12 wt%, AlN was the main inclusion[8]. In the CC process, AlN would float into the slag, increasing viscosity, break temperature, and melting temperature [8, 9], further leading to surface defects. Therefore, to improve the absorption capacity of AlN inclusions by mold flux, it is necessary to explore the dissolution behavior of AlN inclusions in mold flux. In this work, the dissolution behavior of AlN inclusions in CaO–Al_2O_3–BaO–CaF_2–Li_2O slag was investigated by the static experimental method, and the effect of AlN on the properties of slag was studied. This work could lay a theoretical value and reference basis for the design of non-reactive slag for high-Al steel.

Experimental Procedure and Methods

Preparation of Slag Samples and AlN Rods

The composition of the slag used in the experiment is shown in Table 1. The slag samples were prepared using analytical grade chemical reagents, in which Li_2O was prepared in the form of Li_2CO_3. The diameter of AlN rods had a size of Φ10 mm × H10 mm, a density of 95%, and a purity of 99.9%. The AlN powder used in the experiment was an analytical grade chemical reagent with a purity of 99.98%, its oxygen content was less than 0.1 wt%.

Experimental Equipment and Methods

To prevent the AlN rod from being oxidized by the air at high temperatures, the static experiment method which immersed the AlN rods in the slag and isolated them from air was used to explore the dissolution behavior of AlN in the slag, as shown in Fig. 1. 250 g slag sample in Table 2 was prepared and pre-melted at 1300 °C for 20 min in a $MoSi_2$ furnace to uniform the slag composition. Meanwhile, two small graphite

crucibles with AlN rods fixed at the bottom were prepared, and the small graphite crucibles were covered with a large graphite crucible. Subsequently, the pre-melted slag was quickly poured into the small graphite crucibles to completely submerge the AlN rods, and the liquid slag with a height of about 10 mm lower than the top of the small graphite crucibles was poured into the large graphite crucible. The slag in the large graphite crucible did not contact with AlN rods. Besides, a graphite lid was placed on the top of the large graphite crucible to further reduce the oxygen partial pressure in the crucible, and then the large graphite crucible was placed in the furnace at 1400 °C for 1 h and then taken out for air-cooling. Argon was introduced into the experiment to prevent AlN from being oxidized by the oxygen in the air. After that, the slags in the large graphite crucible and the small graphite crucibles were ground through a 200-mesh for XRD detection. The AlN rods after the experiment were cut longitudinally by a diamond wire cutting machine, and then the interface between AlN and slag was analyzed by field emission scanning electron microscope (FE-SEM) after grinding and polishing.

The effects of different AlN additions on the viscosity and melting temperature of slag were tested by rotary viscometer and hemispherical point method, respectively. The experimental equipment and detailed operation process could be found in our previous papers [10–12]. 250 g slag samples were prepared and pre-melted at 1300 °C for 20 min in the furnace to uniform the composition, and then AlN powders were weighed according to 0 wt%, 2 wt%, 4 wt%, 6 wt%, and 8 wt% of the slag sample weight. Thereafter, AlN was added to the surface of the liquid slag utilizing a graphite
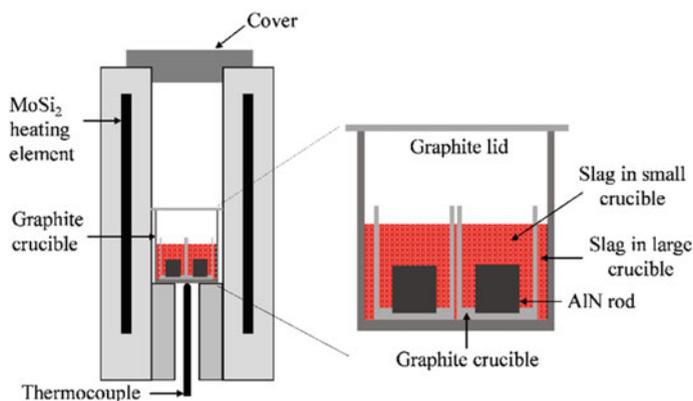
Fig. 1 Schematic of the static slag-AlN rod contacting experiment

Table 2 Compositions of slags after slag-AlN rod contacting experiment (wt%)

Slag samples	CaO	Al$_2$O$_3$	CaF$_2$	Li$_2$O	BaO
NL	30.52	28.29	17.94	7.22	16.03
NS	29.66	32.62	17.30	5.44	14.98

tube. The slag sample was stirred every five minutes to make the added AlN fully react with the fused sample and held at 1300 °C for 0.5 h. Then the furnace was cooled at 6 °C/min to obtain the viscosity and break temperature of the slag. The slag after the viscosity test was ground for melting temperature test. The melting temperature was defined as the temperature at which the height of the slag sample decreased to half of the original height during the test. Each group of samples was tested more than three times, and the mean value of the three groups of test differences not exceeding 10 °C was selected as the melting temperature of the slag. Argon was introduced into the experiment to prevent AlN from being oxidized by the oxygen in the air.

Dissolution Behavior of AlN in the Slag

The Shape Change of the AlN Rod and the Composition Change of the Slag

The longitudinal section shape of the AlN rod stripped from the slag after the dissolution experiments is shown in Fig. 2. It could be noted that the size of the AlN rod was reduced from an initial 10 mm to 7.90 mm, indicating that the slag had a certain ability to dissolve AlN.

The composition of the slag samples in the large graphite crucible and small graphite crucibles is shown in Table 2. The slag was not in contact with the AlN rod in the large crucible and the slag in contact with AlN in the small crucibles was defined as slag NL and NS, respectively. Compared with the original slag, the composition of the slag NL varied from 0.35 to 0.73 wt%, and the contents of CaO, CaF_2, and BaO in the slag NS varied from 0.24 to 0.70 wt%. But remarkably, Al_2O_3 increased by 3.60 wt% and Li_2O decreased by 2.20 wt%. The increase of Al_2O_3 and the decrease of Li_2O in slag NS might be due to the chemical reaction between the slag and AlN rod.

Fig. 2 Shape of AlN rod after experiment

Optical Microscopes and Electrons Microscopic Analysis of Slag-AlN Interface

The slag-AlN interface morphology observed by the optical microscope is shown in Fig. 3. The upper gray part was the slag, and the lower black and white part was AlN. It was evident there was a bright white area at the interface, whose color could be differentiated from that of solidified slags and AlN rods, which may be caused by the reaction between slag and AlN. This part was defined as the interface transition layer between the slag and AlN.

The interface morphology and element surface scanning results of the slag-AlN interface obtained by SEM are shown in Fig. 4, and the element line scanning results of the slag and AlN rod interface are shown in Fig. 5. It can be seen that the AlN rod was in close contact with the slag, and there was obvious mutual penetration of elements at the interface. Al was mainly distributed on the AlN side, Ca and Ba were mainly distributed on the slag side, and there was a small amount of distribution on the AlN side. From the slag side to the AlN side, the concentration of Al increased rapidly, and the concentration of O, Ca, Ba, and F decreased gradually. In general, the N concentration gradually increased from the slag side to the AlN side, although it was higher in some areas of the slag side, which indicated that the reaction occurred at the interface and led to the penetration of the N element at the interface. In addition, the products at the interface near the slag side were Al$_2$O$_3$–CaO–BaO–CaF$_2$ complexes, and the products near the AlN side were individual AlN, Al$_2$O$_3$, and AlN–Al$_2$O$_3$ complexes.

Fig. 3 Interface between slags and AlN rods by optical microscope
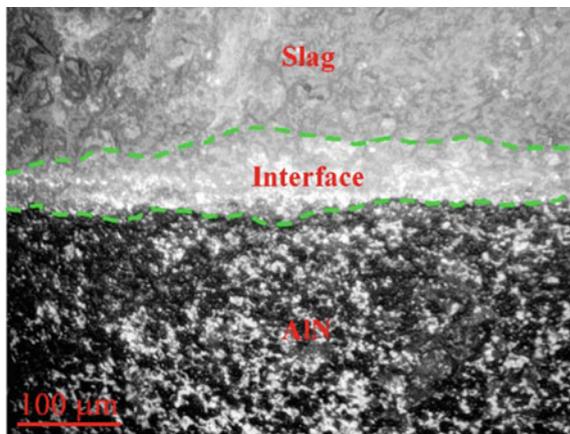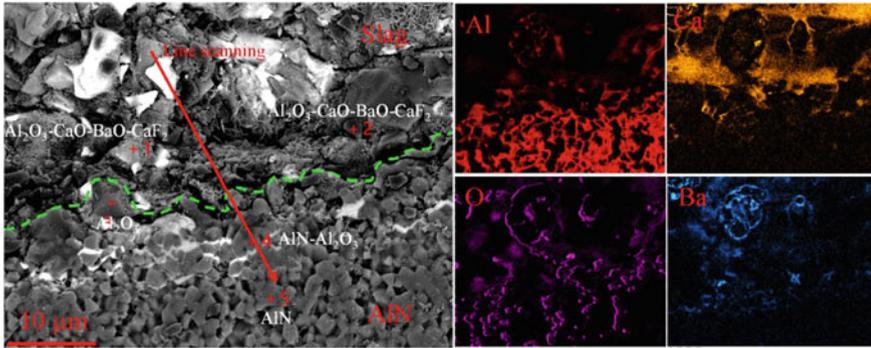
Fig. 4 Interface morphology and elemental mapping of slag and AlN rod

Fig. 5 Line scanning of interface between slag and AlN rod
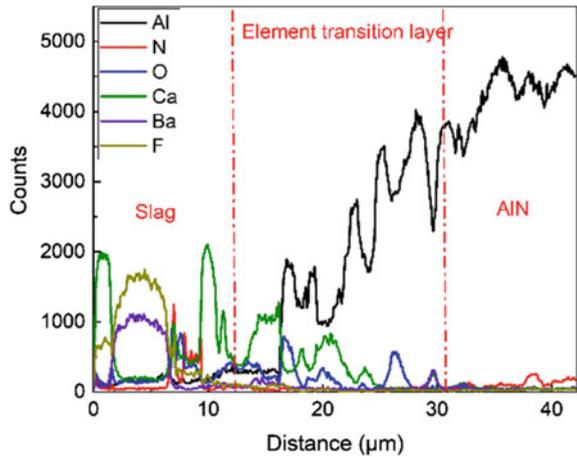
Reactivity Between Slag and AlN

Reactions (1)–(4) are the reactions between AlN and each component, and the Gibbs free energy change formulas of them at 1400 °C calculated by FactSage thermodynamic software are shown in Table 3. It could be seen that AlN only reacted with Li_2O and did not react with others. Therefore, it was reasonable that Al_2O_3 at the interface was formed by the reaction of AlN and Li_2O. AlN or reacted directly with [O] provided by Li_2O to form Al_2O_3, as shown in Reaction (7), or decomposed into [Al] and then reacted with [O] provided by Li_2O to form Al_2O_3 as shown in Eqs. (5), (6) and (8) [13–16]. This was also the reason for the increase of Al_2O_3 and the decrease of Li_2O in the slag which was in contact with the AlN rod after the dissolution experiment.

$$2/3AlN + CaO = 1/3Al_2O_3 + Ca + 1/3N_{2(g)} \tag{1}$$
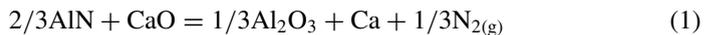
Table 3 Activity of each component in slags at 1400 °C

Slag samples	ΔG_{CaO}	ΔG_{BaO}	ΔG_{Li_2O}	ΔG_{CaF_2}
J/mol	159,392.52	160,804.54	−23,076.96	285,645.01

$$2/3AlN + BaO = 1/3Al_2O_3 + Ba + 1/3N_{2(g)} \tag{2}$$

$$2/3AlN + Li_2O = 1/3Al_2O_3 + 2Li_{(g)} + 1/3N_{2(g)} \tag{3}$$

$$2/3AlN + CaF_2 = 2/3AlF_{3(g)} + Ca + 1/3N_{2(g)} \tag{4}$$

$$AlN = [Al] + 1/2N_2 \quad \Delta G = 282689 - 173T \tag{5}$$

$$AlN = [Al] + 2[N] \quad \Delta G = 303500 - 134.6T \tag{6}$$

$$2AlN + 3[O] = Al_2O_3 + N_2 \quad \Delta G = -679607.5 + 42.5T \tag{7}$$

$$2[Al] + 3[O] = Al_2O_3 \quad \Delta G = -1225000 + 393.8T \tag{8}$$
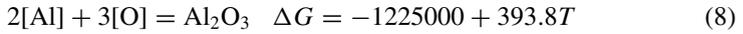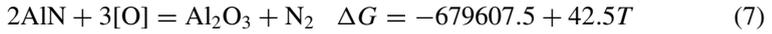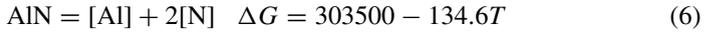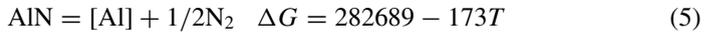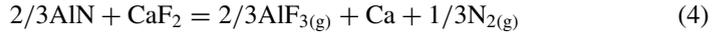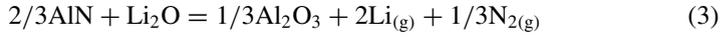
Effect of AlN on the Properties of the Slag

Effect of AlN on Viscosity, Melting Temperature, and Break Temperature of Slag

Figure 6 shows the variation of viscosity, break temperature, and melting temperature of slag with different AlN additions. It can be seen that as the AlN increased, the viscosity of the slag gradually increased from the initial 0.089 to 0.099 Pa s, 0.130 Pa s, 0.176 Pa s, and 0.253 Pa s when 2 wt%, 4 wt%, 6 wt%, and 8 wt% AlN were added. However, the viscosity of the slag was still within the allowable range of CC process. The break temperature (the temperature at which the viscosity of the slag raised sharply during the cooling process) of the slag increased from the initial 1102 to 1145 °C and 1225 °C when 2 wt% and 4 wt% AlN were added. When the amount of AlN added was 6 wt% and 8 wt%, the break temperature decreased by 23 °C and 33 °C, respectively. After absorbing AlN, the break temperature of the slag was too high, which easily led to a decrease in slag consumption, and in turn, caused slab sticking and sticking leakage [17]. In addition, the melting temperature of the slag gradually increased from the initial 1084 to 1159 °C when 6 wt% AlN

(a) viscosity and break temperature   (b) melting temperature
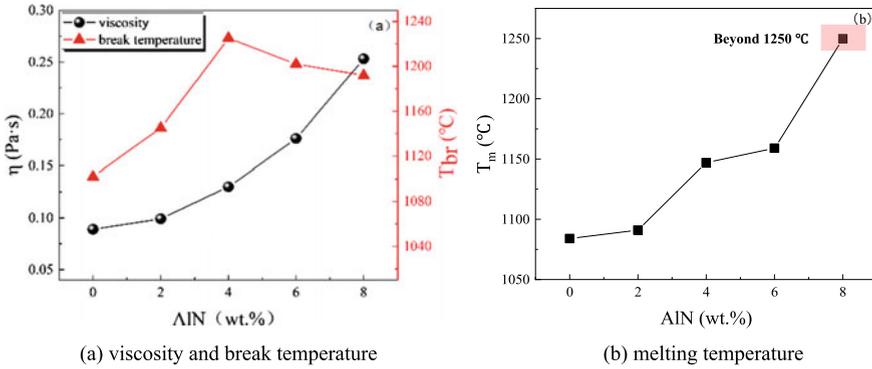
Fig. 6 Basic properties of slag with various AlN additions

was added. When the addition amount of AlN was 8 wt%, the melting temperature of the mold flux exceeded the maximum measured value of 1250 °C allowed by the equipment, which may be due to the formation of high melting temperature phases and gas generation in the slag sample.

Solidification Phase Analyses of Mold Flux

The XRD analysis of the slag samples with varying AlN additions after air-cooling was carried out, as shown in Fig. 7. The initial slag was mainly glass phase with a small amount of $LiBaF_3$. With the addition of AlN in the slag, the precipitated phase in the slag became complicated, in which $11CaO \cdot 7Al_2O_3 \cdot CaF_2$ was the main phase. The melting temperature of $11CaO \cdot 7Al_2O_3 \cdot CaF_2$ was 1577 °C, which would deteriorate the heat transfer controlling and lubrication tasks of solid slag film, it still needs further research

The above experiments on the dissolution of AlN in the slag and the effect of AlN on the properties of slag showed that $CaO–Al_2O_3$-based slag had a certain solubility of AlN, and AlN floated into the slag would deteriorate the slag performance. Under the condition of slag-metal reaction, the performance stability of mold flux was faced with more problems, which required further research on the change of performance of slag after absorbing AlN and its control method.

Fig. 7 XRD analysis of slag with different AlN contents
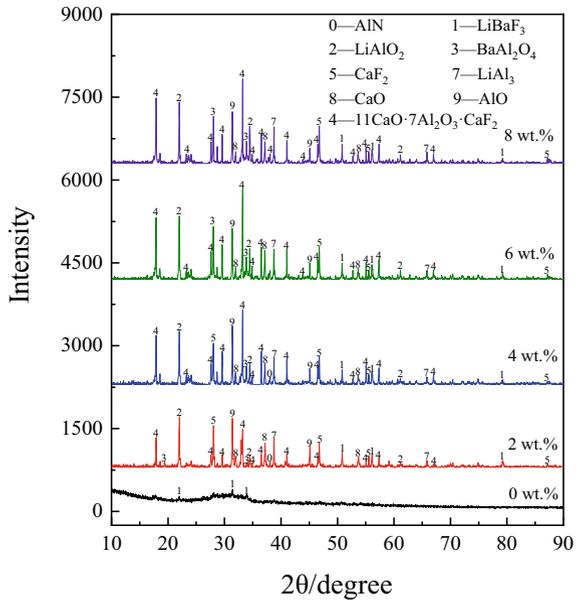
Conclusion

In this study, the dissolution behavior of AlN inclusion in CaO–Al$_2$O$_3$-based non-reactive mold fluxes was explored by SEM–EDS and thermodynamic calculation, and its effect on properties of CaO–Al$_2$O$_3$-based mold flux was also explored. The following conclusions were obtained.

(1) After the dissolution experiment, the content of Al$_2$O$_3$ in the slag contacted with the AlN rod increased by 3.60 wt%, and the content of Li$_2$O decreased by 2.20 wt%.

(2) The results of SEM showed that the product at the slag-AlN interface near the slag side were Al$_2$O$_3$–CaO–BaO–CaF$_2$ complexes, and near the AlN side were individual AlN, Al$_2$O$_3$, and AlN–Al$_2$O$_3$ complexes.

(3) Thermodynamic calculation showed that AlN only reacted with Li$_2$O in slag to produce Al$_2$O$_3$. The dissolution process of AlN inclusions in the slag was inferred as that AlN decomposed to produce [Al] and then reacted with [O] provided by Li$_2$O to produce Al$_2$O$_3$ or AlN directly reacted with [O] provided by Li$_2$O to produce Al$_2$O$_3$.

(4) With the content of AlN in the slag increased from 0 to 8 wt%, the viscosity of the slag increased from 0.089 to 0.253 Pa s, the break temperature increased from 1102 to 1192 °C, and the melting temperature increased from 1084 to 1159 °C when the addition of 6 wt%. When the addition of AlN was 8 wt%, the melting point exceeded 1250 °C.

(5) The XRD result showed that the original slag was mainly glass phase, with the increase of AlN addition, $11CaO \cdot 7Al_2O_3 \cdot CaF_2$ became the main crystalline phase in the slag.

References

1. Tang D, Zhen-Li MI, Chen YL (2005) Technology and research and development of advanced automobile steel abroad. Iron and Steel 40(6):1–5
2. Neu RW (2013) Performance and characterization of TWIP steels for automotive applications. ASTM Int 2(1):20130009
3. Li ZR (2019) Study on reactivity control of mold flux and basic structure and properties of slag for high manganese and high aluminum steel. Chongqing University
4. Wu T, He SP, Guo YT, Wang Q (2014) Study on reactivity between mould fluxes and high-Al molten steel. In: Characterization of minerals, metals, and materials 2014. TMS, San Diego, pp 265–270
5. Chen Y, He SP, Li ZR, Zhang XB, Wang QQ, Wang Q (2022) Properties and structure of a new non-reactive mold flux for high-Al steel. J Iron Steel Res Int 29(1):61–70
6. Chen Y, Pan WJ, Wang QQ, He SP (2022) Study on structure and properties of mold flux for non-reactive high aluminum steel continuous casting. In: The 13th China iron and steel annual conference, Chongqing, China, pp 292–296
7. Yuan HZ, Dan ZK, Wang QQ, He SP (2020) Contact angle and adhesion of $CaO–SiO_2$- and $CaO–Al_2O_3$-based mold slags on solid steel of various compositions. J Market Res 9(4):7828–7837
8. Wang X, Liu H, Zhao M, Wang Q, Zhang X, He S (2023) Effect of AlN on properties of non-reactive $CaO-Al_2O_3$-based mold flux for high-Al steel. Mater Today Commun 34:105432
9. Wang XF, Wang QQ, Zhang XB, Wang Q, He SP (2022) Effect of AlN on properties of $CaO–SiO_2$ based mold flux for high aluminum steel. Iron and Steel 57(05):64–71
10. Li ZR, You XC, Li M, Wang QQ, He SP, Wang QQ (2019) Effect of substituting CaO with BaO and CaO/Al_2O_3 ratio on the viscosity of $CaO–BaO–Al_2O_3–CaF_2–Li_2O$ mold flux system. Metals 9(2):1–13
11. Long X, He SP, Xu JF, Huo XL, Wang Q (2012) Properties of high basicity mold fluxes for peritectic steel slab casting. J Iron Steel Res Int 19(7):39–45
12. Chen Z, Du WT, Zhang M, Wang Q, He SP (2021) Effects of substituting SiO_2 with oxidisers on the reaction performance and physical properties of mould flux for high Ti-bearing steel. ISIJ Int 61(3):814–823
13. Amadeh A, Labbe JC, Laiemeche A, Quintard P (1996) Influence of boron nitride and carbon additives on the behaviour of sintered AlN in a steel-making environment. J Eur Ceram Soc 16(4):403–408
14. Labbe JC, Laïmeche A (1996) Study of the behaviour of aluminium nitride in the iron and steel industry. J Eur Ceram Soc 16(8):893–898
15. Amadeh A, Heshmati-Manesh S, Labbe JC, Laimeche A, Quintard P (2001) Wettability and corrosion of TiN, TiN–BN and TiN–AlN by liquid steel. J Eur Ceram Soc 21(3):277–282
16. Luo Y, Li M, Scheller PR, Sridhar S, Zhang L (2019) Interaction between liquid steel and AlN substrate containing Al-Y-oxides. Metall and Mater Trans B 50(5):2459–2470
17. Mills KC, Fox AB (2003) The role of mould fluxes in continuous casting-so simple yet so complex. ISIJ Int 43(10):1479–1486